Turk J Phys
26 (2002) , 311 – 321.
© TÜBİTAK

Justification of Spherical Approximations using Degree of Linear Polarization of Hot Electron Luminescence from GaAs Crystal

M. N. KHALID*
Optoelectronics Group, Cavendish Laboratory, Madingley Road, Cambridge CB3 OHE, U. K.
e-mail: mnaeemk60@hotmail.com
Shazia YASIN
Microelectronics Research Centre, Cavendish Laboratory, Madingley Road, Cambridge CB3 OHE, U.K.

Received 16.07.2001

Abstract

The anisotropic momentum distribution of photoexcited hot electrons on recombination with holes at the acceptor level produces linearly polarized luminescence. It is found that the degree of linear polarization (DoLP) of the luminescence over the whole width of the first heavy hole peak (0HH) is not constant. Calculations within the spherical approximation show that in bulk GaAs the DoLP over the 0HH peak should vary from zero, at the low energy side, to its maximum value (0.33), at the high energy side of the 0HH peak, for the electric vector of excitation $\hat{\boldsymbol{e}}||[110]$ excitation geometry and vice versa for the $\hat{\boldsymbol{e}}||[100]$ excitation geometry. This variation in the DoLP over the 0HH peak will be referred to as the anisotropy of the DoLP and arises as a direct result of the warping of the heavy hole sub-band. Experimental results were found in qualitative agreement with the calculations under spherical approximation. The calculations within the diagonal approximation could not account for the unexpectedly high value of the DoLP towards the low energy side of the 0HH peak.

1. Introduction

Hot electron luminescence (HEL) spectroscopy is an optical technique that allows the study of electrons in direct gap semiconductors under highly nonequilibrium and steady-state conditions. It analyzes and interprets the emission from hot electrons recombining with states on neutral acceptors. Figure 1 is a schematic of a continuous wave (cw) spectroscopy of hot electrons in GaAs crystal. The continuously active cycle consists of four processes:

1. A laser photon injects electrons from valence states into high energy states in the conduction band.

2. The hot electrons undergo energy and momentum relaxation.

3. During relaxation some electrons combine with neutral acceptors which accompany optical emissions.

4. The ionized acceptors then return the excess electrons to the valence band via acoustic phonons.

*Present address: Physics Department, Islamia College Peshawar, University of Peshawar, Pakistan.

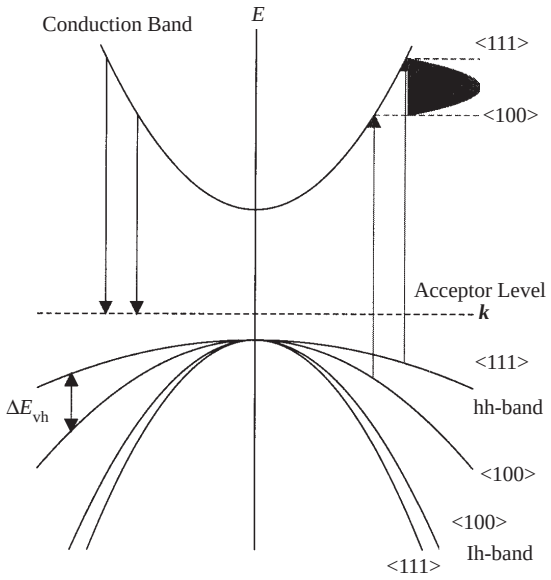

Figure 1. Schematic view of the HEL spectroscopy in lightly p-doped GaAs crystal. The upward arrow represents laser excitation of electrons from the heavy hole band into the conduction band. Relaxation is via emission of a cascade of LO phonons in successive steps of energy $\hbar\omega_{LO}$. The arrows pointing downward represent the recombination of the photoexcited electrons at the acceptor level.

This is a simple process, and interest in it arises from the opportunity that it provides to "monitor" the hot electron population as it relaxes on an ultrafast time scale. From Figure 1 it is straightforward to read the following two energy conservation equations which, respectively, describe the excitation and recombination processes:

$$E_{ex} = E_h(\boldsymbol{k}) + E_0 + E_c(\boldsymbol{k}) \tag{1}$$

$$E_L = E_c(\boldsymbol{k}) + E_0 - E_a \tag{2}$$

where E_{ex} is the laser photon energy, $E_h(\boldsymbol{k})$ and $E_c(\boldsymbol{k})$ are the kinetic energies of the hole and the electron with respect to their band extreme, E_0 is the band-gap, E_a is the acceptor binding energy, and E_L is the energy of the highest luminescence peak in the hot electron cascade.

The luminescence spectrum in Figure 2 shows a cascade structure. This cascade appears due to the scattering of hot electrons by LO phonons. The separation in energy (∼37 meV) between the peaks labeled as 0HH and 1HH etc are on the order of the GaAs LO phonon energy. These are the HEL peaks due to excitation from the heavy hole state, when no phonon (0HH) and one phonon (1HH) are emitted, respectively. Similarly, 0LH is the HEL peaks due to the excitation from the light hole sub-band, when no phonon (0LH) is emitted. The first order Raman peaks, labeled as 1LO is also seen.

As discussed above, the leading peak in the cascade of the heavy hole HEL peaks corresponds to those electrons that have not undergone relaxation by LO phonon emission and its spectral width should arise from three sources [1]:

- An anisotropic valence band
- The acceptor state broadening
- The limited lifetime of the electrons due to the LO phonon emission.

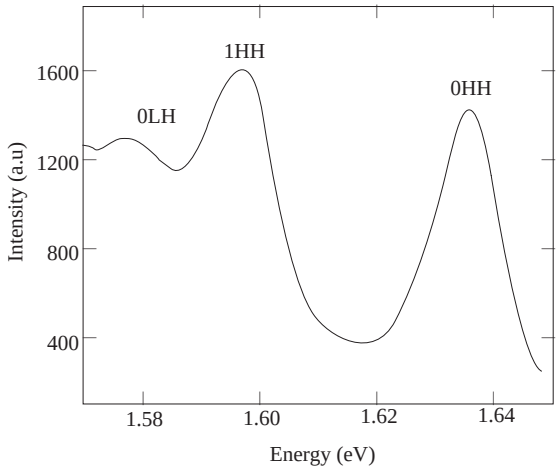

Figure 2. The intensity versus energy graph for hot electron luminescence region. The heavy hole HEL peaks are labelled by HH, and the light hole HEL peaks by LH. The spacing between the consecutive heavy hole peaks (0HH and 1HH) is 37meV, which is nearly equal to the GaAs LO phonon energy.

The focus of the study here is to evaluate the luminescence and hence DoLP along the high symmetry directions; so we will concentrate only on valence band warping. It is the warping in the valence band, which fixes the high symmetry directions in the 0HH peak [2, 3]. The other two factors above will act to broaden the 0HH peak but cannot affect the position of the high symmetry directions in the 0HH peak. The warping in the heavy hole sub-band (light hole sub-band), exists due to the dependence of the effective masses of the heavy holes $m_{hh}\,(m_{lh})$ on the direction of their quasimomentum as shown in Figure 1. The effective masses of the heavy hole along <111> and <100> directions were found to be ∼0.8 and ∼0.4, respectively [4]. Hence the electrons which appear in the conduction band upon monochromatic excitation as a result of the hh-c transition no longer have a monoenergic distribution and instead spread over a band of width of $\Delta\varepsilon_{vh}$. This distribution can be expressed as [4]:

$$\Delta\varepsilon_{vh} = m_c \left[\frac{1}{\left(m_{hh}^{(100)} + m_c\right)} - \frac{1}{\left(m_{hh}^{(111)} + m_c\right)} \right] (\hbar\omega - E_g)\,, \tag{3}$$

where E_g is the band-gap energy; $m_{hh}^{(100)}$, $m_{hh}^{(111)}$ are the heavy hole masses along the <100> and <111> directions; and m_c is the conduction band mass. From Figure 1 it is clear that the high energy sites of the 0HH peak corresponds to the <111> and low energy side to the <100> direction.

Figure 3a shows the cross section through the disc shaped momentum distribution excited by linearly polarised light for $\hat{\boldsymbol{e}}||[010]$. The arrows represent the magnitude of the momenta of the excited electrons from the heavy hole into the conduction band. The arrows have greatest length along the [100] directions and smallest length along the [010] directions. This results in a maximum DoLP at the low energy side of the 0HH peak. As the momentum distribution has a $\sin^2\theta$ shape around the electric vector $\hat{\boldsymbol{e}}$ of the exciting light, the momenta will have identical magnitude along the [110] directions; this produces a minimum value of the DoLP at the high energy side of the 0HH peak [5]. This difference in the DoLP along different directions is what we term the anisotropy of the DoLP. Figure 3b shows the same type of momentum distribution as Figure 3a but this time the electric vector $\hat{\boldsymbol{e}}||[110]$. Following a similar argument, the result in this case is that the DoLP will be at a maximum at the high energy side of the 0HH peak while it is minimal at the low energy side of the 0HH peak. Thus the anisotropy in the DoLP over the 0HH peak exists for both cases of excitation geometries. Using this anisotropy of the DoLP, we will show that spherical approximation is more appropriate to explain HEL characteristics compared to the diagonal approximation.

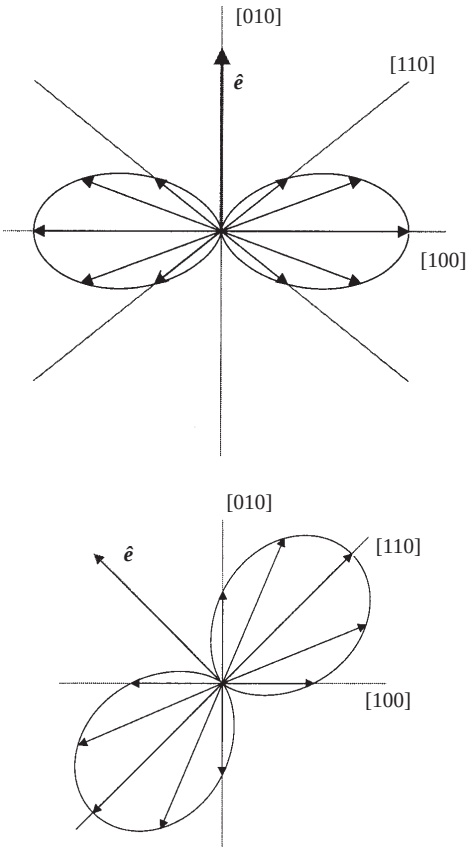

Figure 3. The momentum distribution of the hot electrons excited from heavy hole sub-band for (a) $\hat{e}||[010]$, (b) $\hat{e}||[110]$. The exciting light in both figures is represented by arrows with label $\hat{e}$. The other arrows show the strength of the momenta of the photoexcited electrons in 2D plane. The longer is the arrow, the greater is the number of the photoexcited electrons in that particular direction. Thus (a) most of the electrons are excited with momenta parallel to the <100> and nearly no electron with momenta parallel to the <010>, whereas equal number of electrons are excited with momenta parallel to the <110> and $< 1\bar{1}0 >$, and (b) most of the electrons are excited with momenta parallel to the <110> and nearly no electron with momenta parallel to the $< 1\bar{1}0 >$, whereas equal number of electrons are excited with momenta parallel to the <100> and <010>.

2. Experiment

The hot electron spectroscopy reported in the present work was performed with electrons in the central Γ-valley of GaAs. The excitation energy of 1.6774 eV was achieved with the help of home built Titanium Sapphire Laser pumped by the Coherent Argon Laser and usually works very well to produce a tunable wavelength range of about 790-690 nm, corresponding to 1.57-1.79 eV as an excitation source. In the present work where the polarization characteristics of HEL are investigated, it is extremely essential that the power onto the sample should remain constant. For this purpose Laser Intensity Stabilizer was used, which can produce a stability of 40:1. The experiments were performed with a laser power of ∼9mW. This low power keeps the density of photoelectrons low $\left(2 \times 10^{15}\ cm^{-3}\right)$ to eliminate electron-electron scattering that becomes significant at carrier densities around $10^{17}\ cm^{-3}$ [6].

HEL spectroscopy can only be efficiently performed at low temperatures, where the lattice vibrations are significantly reduced. To achieve low temperatures, a liquid helium cryostat was used (an Oxford Instruments MD10 Bath Cryostat) which has an optical tail fitted with three quartz windows at the level of the spectrometer axis. The samples are cooled by virtue of being attached to a cold finger, which in turn is cooled by vaporizing liquid helium. The temperature of the sample is measured with a Ge-resistor; typically

the sample temperature is 6-8 K without the incident laser beam and up to ∼10K when radiation is incident on the sample.

Spectral measurements were taken using a DILOR XY 0.5m triple monochromator operated in subtractive mode combined with multichannel detection system. The response of the optical elements in the spectrometer dominated by the grating was such that only one direction of linear polarization along the horizontal axis of the laboratory frame was effectively detected. The different polarized components of the luminescence were recorded with the help of single and where ever necessary by the combination of two quarter wave plates that convert any desired polarized component of luminescence into horizontally polarized luminescence.

3. Results and Discussions

3.1. Calculations for the Anisotropy of the DoLP

The anisotropy in the DoLP can best be characterized by the Stokes polarization parameters – the $\mathrm{DoLP}(\boldsymbol{S}_1')$ and the $\mathrm{DoLP}(\boldsymbol{S}_2')$ – calculated along the high symmetry directions [7]. The $\mathrm{DoLP}(\boldsymbol{S}_1')$and $\mathrm{DoLP}(\boldsymbol{S}_2')$ are respectively defined to be the degree of linear polarisation of the luminescence in a particular frame of reference and in a second frame of reference rotated by $\pi/4$ to the initial frame. Although $\mathrm{DoLP}(\boldsymbol{S}_1')$ is sufficient to describe the anisotropy of the DoLP over the 0HH peak, we need to consider $\mathrm{DoLP}(\boldsymbol{S}_2')$ here also so as to monitor the polarisation of the exciting light. The calculations for the $\mathrm{DoLP}(\boldsymbol{S}_1')$ and $\mathrm{DoLP}(\boldsymbol{S}_2')$ are performed within the two standard approximations i.e., the spherical and diagonal approximations. The spherical approximation is based on the assumption that all the $\boldsymbol{k}$-directions contribute equally to the equilibrium holes at the acceptor level, whereas the diagonal approximation assumes that the contribution to the equilibrium holes at the acceptor level is exclusively from the heavy hole sub-band states that posses lowest possible energy. In bulk this corresponds to the <111> directions.

3.1.1. Spherical Approximation

To find the contribution to the luminescence intensity from the high symmetry directions, we use the matrix element for excitation from the valence band to the conduction band $M_{vc}\left(\boldsymbol{k},\hat{\boldsymbol{e}}\right)$, and the matrix element for recombination from the conduction band to the acceptor state $M_{ca}\left(\boldsymbol{k},\hat{\boldsymbol{e}}\right)$. The momentum distribution of the hot electrons produced from the heavy hole sub-band can be shown to be [8]:

$$F\left(\boldsymbol{p}\right)=F_0\left(\boldsymbol{p}\right)sin^2\theta, \tag{4}$$

where θ is the angle between $\hat{\boldsymbol{e}}$ and $\boldsymbol{k}$ and $F_0\left(\boldsymbol{p}\right)$ is the spherically symmetric part of the momentum distribution. $M_{vc}\left(\boldsymbol{k},\hat{\boldsymbol{e}}\right)$, the matrix element of excitation is proportional to $F\left(\boldsymbol{p}\right)$ and is expressed in terms of $\boldsymbol{k}$ and $\hat{\boldsymbol{e}}$ as [9]

$$M_{vc}\left(\boldsymbol{k},\hat{\boldsymbol{e}}\right)\propto 1-\left(\frac{\boldsymbol{k}.\hat{\boldsymbol{e}}}{|\boldsymbol{k}||\hat{\boldsymbol{e}}|}\right)^2. \tag{5}$$

Similarly, the expression for the matrix elements of recombination is:

$$M_{ca}\left(\boldsymbol{k},\hat{\boldsymbol{e}}'\right)\propto 1-\left(\frac{\boldsymbol{k}.\hat{\boldsymbol{e}}'}{|\boldsymbol{k}||\hat{\boldsymbol{e}}'|}\right)^2, \tag{6}$$

where $\hat{\boldsymbol{e}}'$ is the electric vector of the luminescence. The spherically symmetric part $F_0\left(\boldsymbol{p}\right)$ is the same both for excitation and recombination, and is therefore omitted. We can further define the parallel and perpendicular components of the matrix elements of recombination $M_{ca}\left(\boldsymbol{k},\hat{\boldsymbol{e}}'\right)_{||}$ and $M_{ca}\left(\boldsymbol{k},\hat{\boldsymbol{e}}'\right)_{\perp}$ as:

For $\hat{\boldsymbol{e}}'||\hat{\boldsymbol{e}}$,

$$M_{ca}\left(\boldsymbol{k},\hat{\boldsymbol{e}}'\right)=M_{ca}\left(\boldsymbol{k},\hat{\boldsymbol{e}}'\right)_{||}$$

and for $\hat{\boldsymbol{e}}'\perp\hat{\boldsymbol{e}}$,

$$M_{ca}\left(\boldsymbol{k},\hat{\boldsymbol{e}}'\right)=M_{ca}\left(\boldsymbol{k},\hat{\boldsymbol{e}}'\right)\perp.$$

Now, as the luminescence intensity is proportional to the product of the matrix elements for excitation and recombination, the parallel ($I_{||}$) and perpendicular ($I_{\perp}$) components of the luminescence intensity can be written:

$$I_{||}\propto M_{vc}\left(\boldsymbol{k},\hat{\boldsymbol{e}}\right)\times M_{ca}\left(\boldsymbol{k},\hat{\boldsymbol{e}}'\right)_{||} \tag{7}$$

$$I_{\perp}\propto M_{vc}\left(\boldsymbol{k},\hat{\boldsymbol{e}}\right)\times M_{ca}\left(\boldsymbol{k},\hat{\boldsymbol{e}}'\right)_{\perp}. \tag{8}$$

Using Eq. (7) and (8), the DoLP$\left(\boldsymbol{S}_1'\right)$ along the high symmetry directions is calculated using the following formula:

$$DoLP\left(\boldsymbol{S}_1'\right)=\frac{I_{||}-I_{\perp}}{I_{||}+I_{\perp}}. \tag{9}$$

Similarly, the DoLP$\left(\boldsymbol{S}_2'\right)$ along the high symmetry directions is given by:

$$DoLP\left(\boldsymbol{S}_2'\right)=\frac{I_{+45}-I_{-45}}{I_{+45}+I_{-45}}, \tag{10}$$

where

$$I_{+45}\propto M_{vc}(\boldsymbol{k},\hat{\boldsymbol{e}})\times M_{ca}(\boldsymbol{k},\hat{\boldsymbol{e}}')_{\frac{\pi}{4}} \tag{11}$$

$$I_{-45}\propto M_{vc}(\boldsymbol{k},\hat{\boldsymbol{e}})\times M_{ca}(\boldsymbol{k},\hat{\boldsymbol{e}}')_{-\frac{\pi}{4}}, \tag{12}$$

where $M_{ca}\left(\boldsymbol{k},\hat{\boldsymbol{e}}'\right)=M_{ca}\left(\boldsymbol{k},\hat{\boldsymbol{e}}'\right)_{\frac{\pi}{4}}$ for $\hat{\boldsymbol{e}}'||\hat{\boldsymbol{e}}+\pi/4$ and $M_{ca}\left(\boldsymbol{k},\hat{\boldsymbol{e}}'\right)=M_{ca}\left(\boldsymbol{k},\hat{\boldsymbol{e}}'\right)_{-\frac{\pi}{4}}$ for $\hat{\boldsymbol{e}}'||\hat{\boldsymbol{e}}-\pi/4$. DoLP$\left(\boldsymbol{S}_1'\right)$ and DoLP$\left(\boldsymbol{S}_2'\right)$ calculated within this approximation are given in Table 1 and are also shown in Figure 4.

Table 1. The table shows the calculated DoLP within the spherical approximations along the high symmetry directions for GaAs crystals. The excitation geometries used are $\hat{\boldsymbol{e}}||[100]$ and $\hat{\boldsymbol{e}}||[110]$.

DoLP	Wave vector	$\hat{\boldsymbol{e}}\|\|[100]$	$\hat{\boldsymbol{e}}\|\|[110]$
$DoLP\left(\boldsymbol{S}_1'\right)$	<100>	1/4	0
	<110>	1/11	2/11
	<111>	0	1/3
$DoLP\left(\boldsymbol{S}_2'\right)$	<100>	0	0
	<110>	0	0
	<111>	0	0

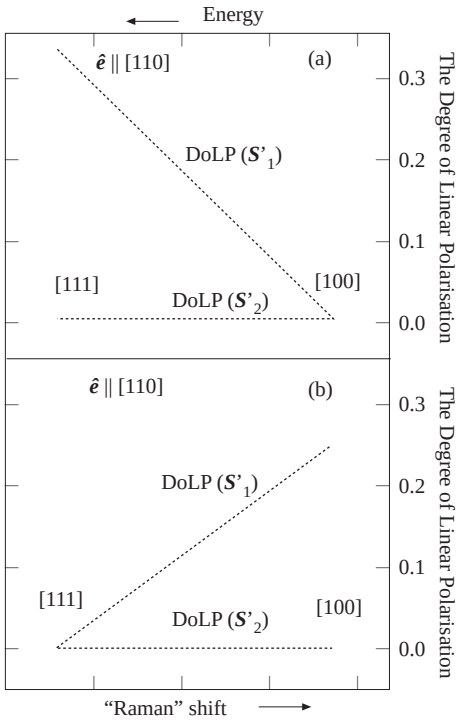

Figure 4. The figure demonstrates the variation in the DoLP($\boldsymbol{S}'_1$) and DoLP($\boldsymbol{S}'_2$) with respect to "Raman" shift over the whole width of the 0HH peak in bulk. The "Raman" shift means the shift towards lower energy taking exciting energy as a reference. The DoLP($\boldsymbol{S}'_1$) is (a) maximum at the high energy side (i.e. the <111> directions) of the 0HH peak and minimum at the low energy side (i.e. the <100> directions) for $\hat{e}$||[110] excitation geometry, (b) minimum at the high energy side and maximum at the low energy side of the 0HH peak for $\hat{e}$||[100] excitation geometry, whereas the DoLP($\boldsymbol{S}'_2$) is zero in both cases of excitation over the whole width of the 0HH peak.

$\mathrm{DoLP}\left(\boldsymbol{S}'_2\right)$ is zero in both cases of excitation. This means that the luminescence intensity along all the directions is the same for $\pi/4\left(I_{||}\right)$ and $-\pi/4\left(I_{\perp}\right)$ with respect to the incident polarization. This is only possible when the incident laser is completely polarized along the stated directions i.e. either [110] or [100]. On the other hand, the $\mathrm{DoLP}\left(\boldsymbol{S}'_1\right)$ is maximal on the high energy side (i.e. the <111> directions) of the 0HH peak and minimum on the low energy side (i.e. the <100> directions) of the 0HH peak for $\hat{e}$||[110] (see Figure 4a).

The anisotropy in DoLP exists because for the $\hat{e}$||[110] excitation geometry, due to the anisotropic momentum distribution, the diagonal directions (i.e. the <111> directions) have a larger contribution to the $I_{||}\left(\hat{e}'||\hat{e}\right)$ component of the luminescence than to the $I_{\perp}\left(\hat{e}'\perp\hat{e}\right)$ component of the luminescence intensity, whereas due to the existence of an isotropic distribution along the principal crystallographic directions (i.e. the <100> directions) the contribution from the <100> directions to both components of the luminescence intensity is identical. For $\hat{e}$||[100] excitation geometry, the anisotropy in the distribution appears along the principal crystallographic directions and the distribution becomes isotropic along the diagonal directions, thus $\mathrm{DoLP}\left(\boldsymbol{S}'_1\right)$ is larger on the low energy side than on the high energy side of the 0HH peak (Figure 4b).

3.1.2. Diagonal Approximation

The calculated polarisation characteristics of the 0HH peak changes significantly when the calculations are performed within the diagonal approximation. This approximation assumes that for low temperature, the distribution of equilibrium holes is highly anisotropic and the recombination is exclusively governed by the holes whose quasimomentum is parallel to the diagonal directions i.e. the <111> directions. Using the expressions for the matrix elements (Equations (5) and (6)) with the constraint that apart from the diagonal directions, no other directions can contribute to the luminescence, the $\mathrm{DoLP}\left(\boldsymbol{S}'_1\right)$ and the $\mathrm{DoLP}\left(\boldsymbol{S}'_2\right)$ are calculated and are given in Table 2.

Table 2. The values of the DoLP calculated within the diagonal approximation along the high symmetry directions for GaAs crystal are shown. All the calculations are performed for two cases of excitation geometries i.e. $\hat{\boldsymbol{e}}||[100]$ and $\hat{\boldsymbol{e}}||[110]$.

DoLP	Wave vector	$\hat{\boldsymbol{e}}\|\|[100]$	$\hat{\boldsymbol{e}}\|\|[110]$
$DoLP\left(\boldsymbol{S}_1'\right)$	<100>	0	0
	<110>	0	0
	<111>	0	1/3
$DoLP\left(\boldsymbol{S}_2'\right)$	<100>	0	0
	<110>	0	0
	<111>	0	0

Note that the luminescence for $\hat{\boldsymbol{e}}||[100]$ is unpolarised ($\mathrm{DoLP}\left(\boldsymbol{S}_1'\right) = 0$); this is because all the diagonal directions are equivalent and populated identically, just as if the distribution function was isotropic. The maximum value of the $\mathrm{DoLP}\left(\boldsymbol{S}_1'\right)$ for $\hat{\boldsymbol{e}}||[110]$ arises because in this excitation geometry, the momentum distribution is highly anisotropic along the diagonal directions, which are the only directions contributing to the luminescence intensities.

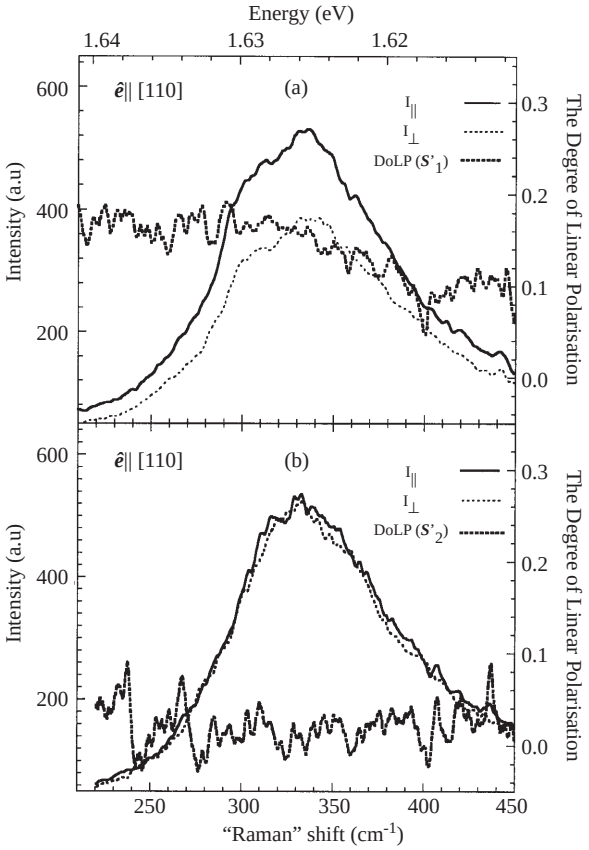

Figure 5. The luminescence intensities ($I_{||}$ and $I_{\perp}$) and the (a) $\mathrm{DoLP}\left(\boldsymbol{S}_1'\right)$ and (b) $\mathrm{DoLP}\left(\boldsymbol{S}_2'\right)$ for $\hat{\boldsymbol{e}}||[110]$ excitation geometry. The $\mathrm{DoLP}\left(\boldsymbol{S}_1'\right)$ is minimum at the low energy side and maximum at the high energy side of the 0HH peak, whereas the $\mathrm{DoLP}\left(\boldsymbol{S}_2'\right)$ is zero over the whole width of the 0HH peak [10].

3.2. Comparison of Experimental results and Calculations

Figures 5 and 6 show the experimentally obtained luminescence intensities and the Stokes parameters i.e. the $\mathrm{DoLP}\left(\boldsymbol{S}_1'\right)$ and $\mathrm{DoLP}\left(\boldsymbol{S}_2'\right)$ for $\hat{\boldsymbol{e}}||[110]$ and $\hat{\boldsymbol{e}}||[100]$ excitation geometries, respectively. The variation

of the DoLP$\left(\boldsymbol{S}_1'\right)$ for $\hat{\boldsymbol{e}}$||[110] over the 0HH peak is clearly evident in Figure 5a. It can be seen that the DoLP$\left(\boldsymbol{S}_1'\right)$ has a maximum value of 0.15 on the high energy side and has a minimum value of 0.02 on the low energy side of the 0HH peak [10].

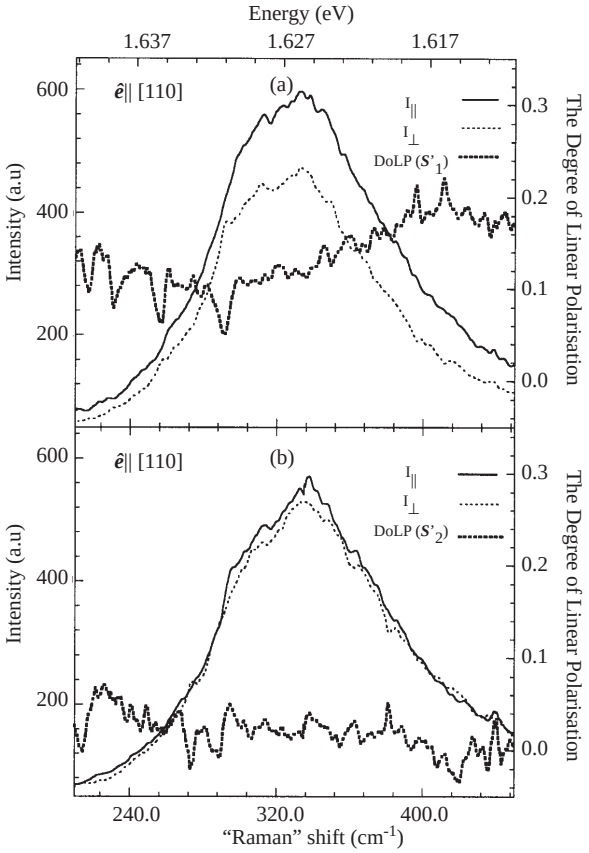

Figure 6. The luminescence intensities ($I_{||}$ and $I_{\perp}$) and the (a) DoLP($\boldsymbol{S}_1'$) and (b) DoLP($\boldsymbol{S}_2'$) for $\hat{\boldsymbol{e}}$||[100] excitation geometry. The DoLP($\boldsymbol{S}_1'$) is maximum at the low energy side and minimum at the high energy side of the 0HH peak, whereas the DoLP($\boldsymbol{S}_2'$) is zero over the whole width of the 0HH peak [10]

Figure 5b shows that the DoLP$\left(\boldsymbol{S}_2'\right)$ is nearly zero over the whole width of the 0HH peak for $\hat{\boldsymbol{e}}$||[110] excitation geometry which shows that the electric vector $\hat{\boldsymbol{e}}$ of the incident light is precisely parallel to the crystallographic axis [110]. The experimental variation of the DoLP$\left(\boldsymbol{S}_1'\right)$ over 0HH peak for the electric vector of the excitation light parallel to the direction [100] is shown in Fig. 6a. On the low energy side of the 0HH peak (i.e. the <100> directions), the DoLP$\left(\boldsymbol{S}_1'\right)$ reaches its maximum value of 0.22 and drops to 0.12 towards the high energy side of 0HH peak (i.e. the <111> directions). The DoLP$\left(\boldsymbol{S}_2'\right)$ (Figure 6b) remains nearly zero over the entire width of the 0HH peak showing that the incident light is polarised parallel to the [100] axis.

The diagonal approximation is able to qualitatively explain the variation of the DoLP$\left(\boldsymbol{S}_1'\right)$ and the DoLP$\left(\boldsymbol{S}_2'\right)$ for $\hat{\boldsymbol{e}}$||[110] excitation geometry and also DoLP$\left(\boldsymbol{S}_2'\right)$, for $\hat{\boldsymbol{e}}$||[100] excitation geometry but does not satisfactorily account for the DoLP$\left(\boldsymbol{S}_1'\right)$ on the low energy side of 0HH peak, when the incident light is polarized parallel to the [100] direction. This is because this approximation assumes that no other directions contribute to the luminescence but the diagonal directions. To demonstrate that other directions also contribute to the luminescence intensity, Kash [11] and later Hackenberg [12] plotted the difference spectrum $I_{||} - I_{\perp}$ for $\hat{\boldsymbol{e}}$||[100] excitation geometry shown in Figure 7. The appearance of a peak on the low energy side of the 0HH peak in the difference spectra was taken as a proof of the contribution to luminescence by the <100> directions.

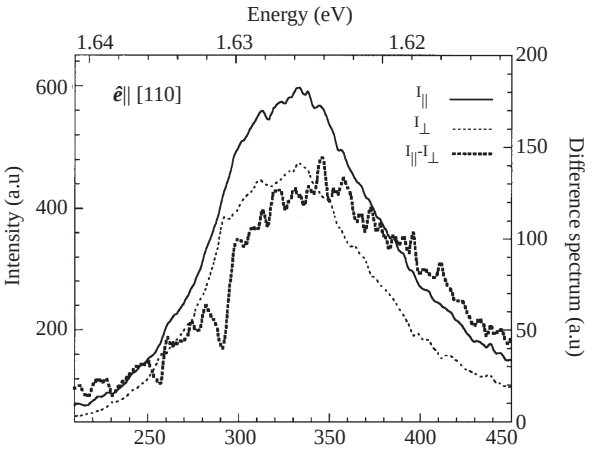

Figure 7. The luminescence intensities ($I_{||}$ and $I_{\perp}$) and the difference spectrum ($I_{||} - I_{\perp}$) for $\hat{e}||[100]$ excitation geometry. The difference spectrum shows a peak at the low energy side of the 0HH peak, showing the contribution from the <100> directions in the luminescence.

There is, however, a qualitative agreement between the experimental data for the $\mathrm{DoLP}(\boldsymbol{S}'_1)$ and the $\mathrm{DoLP}(\boldsymbol{S}'_2)$ (Figures 5 and 6) and the results of the calculations for the $\mathrm{DoLP}(\boldsymbol{S}'_1)$ and the $\mathrm{DoLP}(\boldsymbol{S}'_2)$ within the spherical approximation for both excitation geometries; the quantitative disagreements can be explained by noting that the luminescence intensity obtained experimentally exhibits contributions from photoexcited electrons in all $\boldsymbol{k}$-directions, while the calculations are performed by considering the contributions to the luminescence intensities only from the high symmetry directions. On the basis of this, we conclude that the spherical approximation is more appropriate than the diagonal approximation for explaining the HEL characteristics from bulk GaAs. It is also found (but not present in here) that spherical approximation can reasonably explain the HEL characteristics from quantum well structures under some special condition.

4. Conclusion

The calculations for the anisotropy of the DoLP over the 0HH peak for bulk material are performed within the spherical and diagonal approximations. Calculations within the spherical approximation were found in qualitative agreement with the experimental results. The applicability of the diagonal approximation is questioned because of the presence of a peak in the difference spectrum for the $\hat{e}||[100]$ excitation geometry. Thus it was concluded that the spherical approximation is more appropriate to explain HEL characteristics in bulk materials.

References

[1] B. P. Zakharchenya, D. N. Mirlin, V. I. Perel and I. I. Reshina, *Uspekhi Fizicheskikh Nauk* **36**, (1982) 459.

[2] J. A. Kash, M. Zachau, M. A. Tischler and U. Ekenberg, *Phys. Rev. Letters* **69**, (1992) 2260.

[3] W. Hackenberg, Ph. D. Thesis, University of Cambridge (1993).

[4] V. D. Dymnikov, D. N. Mirlin, V. I. Perel and I. I. Reshina, *Sov. Phys. solid State* **20**, (1978), 1250.

[5] M. A. Alekseev, I. Y. Karlik, I. A. Merkulov, D. N. Mirlin and V. F. Sapega, *Phys. Letter A* **127**, (1988), 373.

[6] J. A. Kash, *Phys. Review B* **40**, (1989), 3455.

[7] M. N. Khalid, *Ph.D. thesis, University of Cambridge* (2000).

[8] V. D. Dymnilov, M. I. D'yakonov and N. I. Perel, *Sov. Phys. JETP* **44**, (1976) 1252.

[9] G. Fasol, W. Hackenberg, H. P. Hughes, K. Ploog, E. Bauser, H. Kano, *Phys. Rev. B* **41**, (1990), 1461.

[10] J. P. Evans, V. Saxena, H. P. Hughes *Physica Status Solidi B-Basic Research,* **204**, (1997) 125.

[11] J. A. Kash, *Phys. Rev. B* **47**, (1993) 1221.

[12] W. Hackenberg and H. P. Hughes, *Phys. Rev. B* **49**, (1994) 7990.